A new machine vision real-time detection system for liquid impurities based on dynamic morphological characteristic analysis and machine learning

Li, Xinyu; Qiao, Tiezhu; Pang, Yusong; Zhang, Haitao; Yan, Gaowei

DOI
10.1016/j.measurement.2018.04.015

Publication date
2018

Document Version
Final published version

Published in
Measurement

Measurement 124 (2018) 130–137

Contents lists available at ScienceDirect

Measurement

journal homepage: www.elsevier.com/locate/measurement

A new machine vision real-time detection system for liquid impurities based on dynamic morphological characteristic analysis and machine learning

Xinyu Li[a,b], Tiezhu Qiao[a,b,*], Yusong Pang[b,c,*], Haitao Zhang[a,b], Gaowei Yan[d]

[a] Engineering Research Centre for Measuring and Controlling Technology and Advanced Transducers of Shanxi Province, Taiyuan University of Technology, Taiyuan 030024, China
[b] Institute of Measuring and Controlling Technology of Taiyuan University of Technology, Taiyuan 030024, China
[c] Section of Transport Engineering and Logistic, Faculty of Mechanical, Maritime and Materials Engineering, Delft University of Technology, 2628 CD Delft, Netherlands
[d] College of Information Engineering, Taiyuan University of Technology, Taiyuan 030024, China

ARTICLE INFO

Keywords:
Machine vision
Liquid impurity detection system
Dynamic morphological characteristic
K-Nearest Neighbor (KNN) machine learning

ABSTRACT

Impurity in transparent-bottled liquid is a serious production accident in the field of beverage and medicine industry. However, the existing detection systems are difficult to distinguish impurities with dynamic interference (bubbles and stains) and detect impurities located at the edge of the bottle. In order to solve the problems stated above, a new machine vision system for detecting tiny and dynamic impurities is proposed in this paper. In the system, circularity calculation, longitudinal frame-difference method, orthogonal-axis inspection and K-Nearest Neighbor (KNN) machine learning algorithm are combined together to realize the automatic and real-time detection. Experimental results demonstrate that, after completing machine learning, the weighted error of the proposed system for detecting impurities can be effectively controlled at about 0.9% even in dynamic interference environment, which is great significance to safety production in beverage and medicine industry.

1. Introduction

Beverage and medicine industry is an important part of industrial production. Transparent-bottled liquid accounts for a great proportion in the whole products of beverage and medicine industry [1]. In the process of liquid production, inevitably, some transparent-bottled liquid may include impurities, such as floc (indicating that the liquid has gone bad), residue (indicating a filtration system error) and glass fragment (directly damaging the human body). Therefore, detection of impurities is of great significance for production safety in beverage and medicine industry.

However, impurity detection is mainly based on manual-visual inspection traditionally, which is time-consuming and inefficient. Especially in the situation of long working hours (about 2 h), serious discomfort with visual deterioration and impaired concentration may occur to inspectors, which overwhelmingly damages the quality of impurity inspection and the health of workers. With the development of automatic detection technologies, a series of automatic inspection systems have been proposed based on High Performance Liquid Chromatography (HPLC) by researchers [2–4], which have a satisfactory performance. However, the HPLC systems are difficult to realize real-time impurity detection of products on assembly line.

Because of the advantages of stability, accuracy and cheapness [5–9], machine vision has become one of the development tendencies for impurity detection, and a great many of detection systems have been proposed. Huang, Li, Wang, et al., have proposed a least squares filtering detection system [10], which uses least squares filtering algorithm to obtain low noise images, and take the closed pattern in the image as impurity. Huang, Ma, Lv, et al., have proposed a fuzzy least squares support vector machine system [11], which uses fuzzy least squares support vector machine to recognize the impurities which are similar with bubbles. However, the least squares filtering detection system is hard to distinguish impurities and dynamic bubbles, and fuzzy least squares support vector machine system may misjudge the stains on the surface of bottle as impurities. Besides, impurities at the edge of bottles (the impurity images may become deformed) is difficult to be recognized in the existing impurity detection systems.

In this paper, a new real-time detection system for impurities in transparent-bottled liquid is proposed based on machine vision. The system combines technologies such as circularity calculation, longitudinal frame-difference method, orthogonal-axis inspection and K-Nearest Neighbor (KNN) machine learning algorithm to solve the problems in existing detection systems.

1. The orthogonal-axis inspection method uses two CCD cameras, the optical axes of which are configured to be orthogonal so that at least

* Corresponding authors at: Institute of Measuring and Controlling Technology of Taiyuan University of Technology, Taiyuan 030024, China.
E-mail address: lixinyu0951@link.tyut.edu.cn (T. Qiao).

https://doi.org/10.1016/j.measurement.2018.04.015
Received 25 October 2017; Received in revised form 5 April 2018; Accepted 6 April 2018
Available online 07 April 2018

one camera captures the undeformed image of impurity at the same time.
2. The circularity calculation calculates the circularity of every closed pattern, which is able to separate tiny impurities from bubbles.
3. The longitudinal frame-difference operation identifies all objects that have longitudinal motion components, which is responsible for distinguishing impurities and stains on the surface of bottles.
4. By contrasting with the database, K-Nearest Neighbor (KNN) machine learning algorithm determines whether there is any impurity in the detected sample, which can improve adaptability of the system in complex detection environment.

On the experimental platform in the laboratory, massive experiments are carried out to test the impurity detection effectiveness of the system. Experimental results demonstrate that, after completing machine learning, the weighted error of the designed system for detecting impurities with dynamic interference is about 0.9%.

In this paper, Section 2 describes the principle of digital image processing method (circularity calculation, longitudinal frame-difference method and orthogonal-axis inspection) used in the system. Section 3 represents the mathematical model of KNN machine learning algorithm and the effect of this algorithm. Section 4 illustrates the structure and detection process. Sections 5 and 6 individually display experimental scheme & results and conclusion.

2. Visual recognition method

In the actual detection environment, the kinestate of detected samples can be divided into two stages–rotation and translation. In the process of rotation, the samples rotate 180 degrees quickly in vertical direction, which stirs the impurities contained in the samples and improves the accuracy of impurities identification. However, a large number of bubbles may appear in the liquid when the impurities are stirred. In the process of translation, samples are measured horizontally in constant speed, yet stains on the surface of samples may be misjudged as impurities. Besides, impurities at the edge of bottles are really difficult to be detected because of the deformation of them. In this paper, the digital image processing method of the designed system can filter out above interference effectively.

2.1. Circularity calculation

Circularity calculation is able to realize separation of impurities and stains from bubbles in the field of morphology [12–15]. Impurities in bottled liquid are mainly composed of flocs, glass ballast and food debris, meanwhile the stains attached to the surface of samples are mainly composed of glue marks, glass cracks and dust. The commonness of above impurities and stains is that they are all irregular shapes in the detection images. By contrast, bubbles in detection images are regular circles because of the minimal volume. The different morphological features of impurities/stains and bubbles are shown in the Fig. 1. In this paper, the calculated circularity is used as a reference standard to distinguish impurities/stains and bubbles in the process of detecting impurity.

The formula of calculating circularity is shown as follows.

$$C = \frac{4\pi A}{P^2} \tag{1}$$

In formula, C is the circularity of geometric figures, A is the area of geometric figures, and P is the perimeter of geometric figures.

The laboratory has received about 50 random impurity samples (the impurity samples and the qualified samples each account for half) provided by the cooperative enterprise and measured the circularity of impurities and bubbles successively. The measuring results show that the circularity of most impurities and stains is within the range of 0.1–0.5, meanwhile the circularity of subtotal bubbles is within the range of 1.0–1.3. The circularity difference of impurities and bubbles is shown in Fig. 2.

Based on the above principle, circularity calculation method can effectively avoid error detection in case of impurities mixing with a large number of bubbles. Circularity and area from circularity calculation are involved in machine learning as important parameters.

2.2. Longitudinal frame-difference algorithm

Longitudinal frame-difference algorithm realizes separation of impurities and stains on the surface of bottles in the field of kinematics. Transparent bottles on assembly lines are occasionally scratched and stained. Most stains attached to the surface of bottles are hardly to be distinguished from impurities only based on their morphological characteristics.

Different from the traditional frame-difference method, this paper merely detects objects with longitudinal motion component by frame-difference operation.

The formula of longitudinal frame-difference method is as follows.

$$T(k) = A(k) - B(k) \tag{2}$$

In this formula, $A(k)$ and $B(k)$ are longitudinal location-component vectors of objects conforming circularity constraints in two consecutive-detected images. $T(k)$ is longitudinal motion-component vectors of objects, which conforming circularity constraints. And $T(k)$ is involved in machine learning as an important parameter.

2.3. Orthogonal vision inspection

After overturning of bottle, impurities may be anywhere in bottles and move irregularly with liquid. Once they are excessively close to the side of glass bottles, they may become deformed or even disappeared in detection images because of the refraction and reflection of light.

Therefore, an orthogonal vision inspection method is proposed. The optical axes of two HR CCD cameras are arranged orthogonally. The main CCD camera is responsible for shooting the side of glass bottles; meanwhile, the auxiliary CCD camera is responsible for shooting the other side of glass bottles. The impurities missed by the main CCD camera can be captured by the auxiliary CCD camera. In Fig. 3, the image of main camera does not contain any impurity, however, there is an obvious impurity in the image of auxiliary camera, which can effectively avoid the vision blind area of the main camera.

Specifically, as shown in Fig. 4, the two HR CCD cameras are immobilized at the side of samples, whose optical axes are orthogonal to each other. The edge positions of samples captured by main camera are at the central positions in camera B. The orthogonal vision inspection guarantees that at least one CCD camera obtains images of the undeformed impurities, thus the problem of deformed impurity recognition can be solved effectively.

3. Machine learning based on K-Nearest Neighbor

Traditionally, the detection systems realize the identification of impurities by artificially determining the threshold of sensitive parameters. However, the threshold segmentation method is too subjective to adapt to complex detection environment (parameters such as illumination, shape of samples, and movement state of samples vary all the time). Subsequently, some dynamic adjustment algorithms were proposed for determining the threshold. Yet a single-deterministic threshold is unable to satisfy the increasing accuracy requirement of detection systems. Therefore, the K-Nearest Neighbor (KNN) machine learning algorithm is adopted to discriminate impurities because of its satisfactory parameter clustering performance [16–19].

Identifying impurities requires three key parameters: circularity, area and longitudinal motion component. Each parameter can form a parameter vector independently. Because the parameters are

(a) (b) (c)

Fig. 1. The different morphological features of (a) impurities, (b) stains and (c) bubbles.

(a) (b)

Fig. 2. The circularity difference of (a) impurities and (b) bubbles.

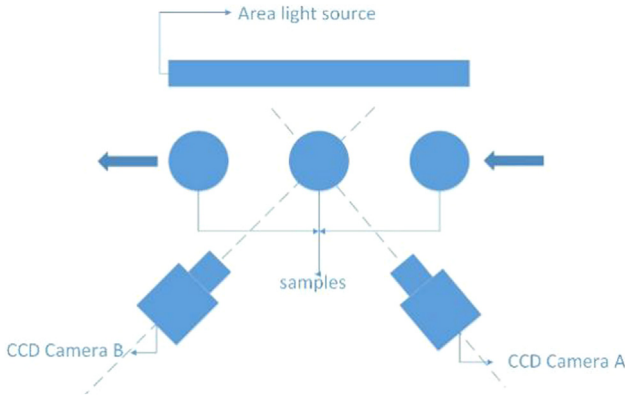

Fig. 4. Diagram of orthogonal vision inspection.

independent of each other, thus the three parameter-vectors can be orthogonal to each other for forming a three-dimensional parameter-space. In the process of machine learning, the training-samples are arranged according to the method of impurity/non-impurity. Every detected training samples can extract three parameter-coordinates, thus every sample can have a unique-determined position in the parameter-space. The aggregation condition of every key parameter is shown in the Fig. 5. In Fig. 5, there are three aggregation regions in the parameter space, which respectively indicate impurities (low circularity, small area and high longitudinal displacement), bubbles (high circularity, small area and high longitudinal displacement), and stains on the surface of transparent bubbles (low circularity, big area, and low longitudinal displacement). Through extensive samples training, three

(a) (b)

Fig. 3. Effect of orthogonal vision inspection image of (a) main CCD camera and (b) auxiliary CCD camera.

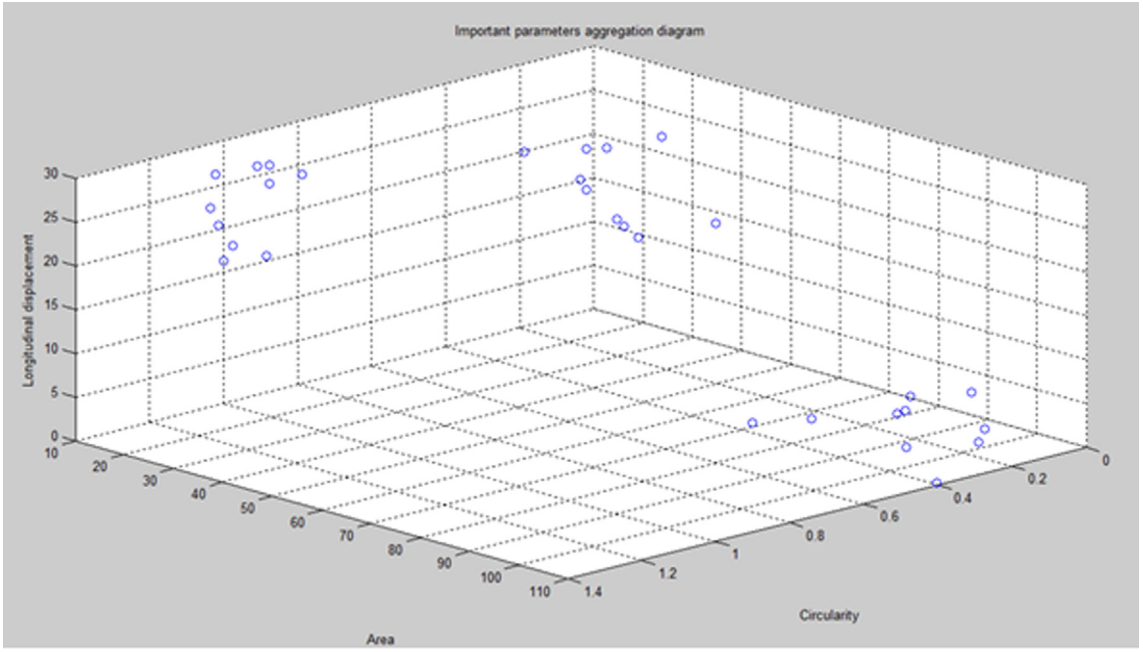

Fig. 5. Three aggregation regions in the parameter space.

aggregation regions are increasingly apparent within the parameter-space. After machine learning, the standard of judging impurities can be determined by the correlation between the parameter-coordinate of samples and the aggregation regions.

Concretely, the correlation between the parameter-coordinate of samples and the aggregation regions is the distance between new sample parameter-coordinates and the geometric center of the aggregation domain regions. The geometric center is determined by K-means clustering algorithm [20–22]. The detailed description of the K-mean algorithm is as follows.

1. In the parameter space, the existing sample parameter coordinates are $\{a_1,a_2,...,a_n\}$, $a_i \in R^3$. From KNN algorithm, exactly, there are 3 aggregation regions (clusters) in the parameter space. Therefore, 3 cluster centroids are randomly selected (In principle, selecting existing parameter points), which are $\{\mu_1, \mu_2, \mu_3\}$, $\mu_i \in R^3$.
2. $\{c_1, c_2, c_3\}$ are 3 clusters in the parameter space, indicating impurity, bubble and stain. The formula for determining which cluster the sample parameter- coordinate belongs to is shown as follows.

$$c_i := \arg\min_j \|a_i - \mu_j\|^2 \tag{3}$$

According to the existing clusters, the formula for determining new cluster centroid is shown as follows.

$$\mu_j = \frac{\sum_{i=1}^{m} 1\{c_i = j\} a_i}{\sum_{i=1}^{m} 1\{c_i = j\}} \tag{4}$$

The new cluster centroids can gradually converge to actual centroids with the process of persistently repeating formula (3) and (4). It is worth noting that, in the process of impurity detection, new sample parameters are continually added to the clusters. The new added sample may cause movement of the original cluster centroids. The formula for calculating new cluster centroid after adding new sample is shown as follows.

$$\begin{cases} x_2 = x + \frac{x - x_1}{N\sqrt{M}} \\ y_2 = y + \frac{y - y_1}{N\sqrt{M}}, \quad (\ \mathrm{M} = (x - x_1)^2 + (y - y_1)^2 + (z - z_1)^2 \\ z_2 = z + \frac{z - z_1}{N\sqrt{M}} \end{cases} \tag{5}$$

$B(x, y, z)$ is the original centroid, and $B_1(x_1, y_1, z_1)$ is the new sample parameter. N is the existing sample size. $B_2(x_2, y_2, z_2)$ is the new cluster centroid.

With the increasing number of sample size of clusters, the detection accuracy of KNN machine learning algorithm is constantly improved. Experimental result shows that the KNN machine learning algorithm completely eliminates subjective interference in impurity detection, and it is able to adapt to a variety of complex detecting environment.

4. System design

Design of the impurity detection system can be divided into two parts: hardware and process.

4.1. Hardware design

The system is composed of three parts: image acquisition subsystem, impurities detection subsystem, alarm and control subsystem. The image acquisition subsystem consists of large area light source (MINDVISION, 500 mm * 300 mm), infrared trigger switch, and HR (high resolution) CCD camera (IMAGINGSOURCE, 10 million pixels). The impurities detection subsystem consists of IPC (industrial personal computer, I7 7700HQ, 8G memory) and central monitor (DELL). The alarm and control subsystem consists of PLC (SIEMENS, S7-200) and ejecting mechanical device (MTSCITECH). The image acquisition subsystem is installed on both sides of assembly lines; meanwhile, the alarm and control subsystem is installed at the downstream position of the image acquisition subsystem. The IPC is installed in the central control room which is adjacent to the production workshop. The installation of system is shown in Fig. 6.

4.2. System process

The large area light source provides adequate illumination for glass bottles and highlights the characteristics of impurities. The CCD cameras are responsible for capturing impurities in bottled liquid images when receiving rigger signal from infrared trigger switch. Subsequently, the HR CCD camera transmits impurities images to IPC. After receiving impurities images, IPC judges whether there are impurities in detected glass bottles based on the correlation between the sample parameter

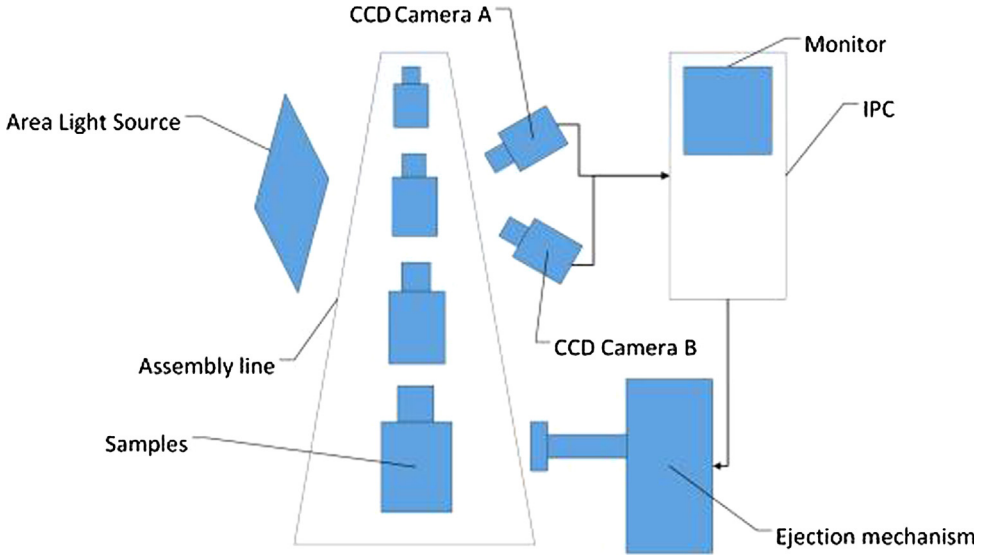

Fig. 6. Installation of the whole system.

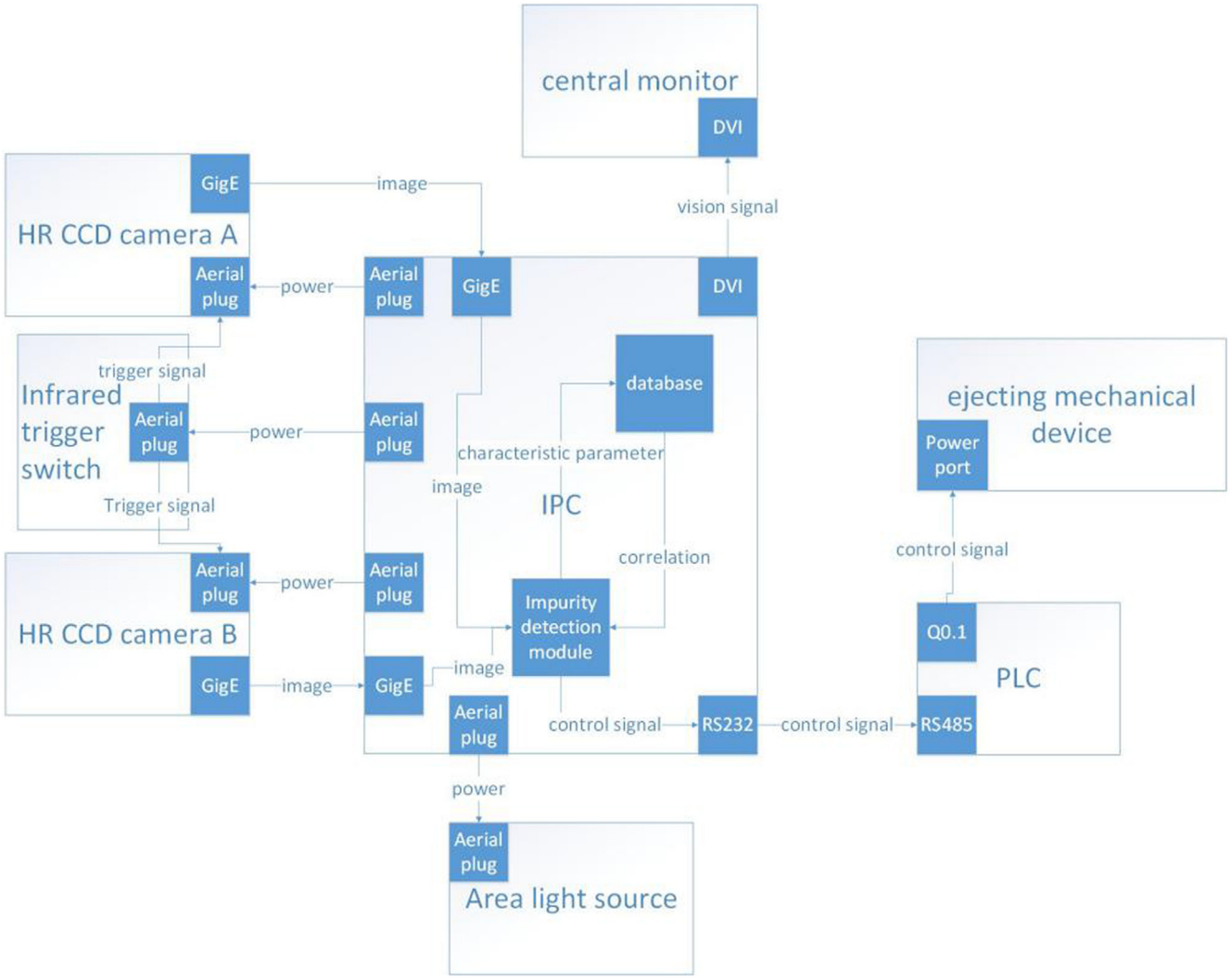

Fig. 7. Structure diagram of the whole system.

Fig. 8. The testing platform.

and the aggregation regions in database, and adds sample parameters to the database. Meanwhile, IPC displays detection results on the central monitor in real time. The alarm and control subsystem takes ejection or hold operation to detected glass bottle based on control signal from IPC. The structure diagram of whole system is shown in Fig. 7.

5. Experiments

Experiments are carried out to test and verify the performance of designed system. The testing platform is shown in Fig. 8. The experimental design, results and limitation analysis are described as follows.

5.1. Experimental design and results

In order to simulate the actual assembly line as much as possible, a sample carrier platform (turntable) is set up in the laboratory, which can achieve all the basic actions of the assembly line. There are 6 sample brackets on the sample carrier and brackets are numbered from No. 1 to No. 6 successively. The No. 1, No. 3 and No. 5 brackets are installed impurity samples, the No. 2, No. 4 and No. 6 brackets are installed qualified samples, and almost every sample contains bubbles and stains. In the process of experiment, existence of minimal probability, the detection system may misjudge the qualified samples as impurity samples (vice versa). Therefore, the designed experiment will focus on measuring the error of each sample individually and the above error is used as the core reference index to evaluate the performance of the designed system. In addition, because samples on the turntable are difficult to be ejected by mechanical device, thus the ejection mechanical device is replaced by a warning light in the experiment.

Before the test begins, the IPC invokes the large area light source, HR CCD camera, infrared trigger switch and returns self-inspection report. After confirmation, the assembly line starts and the whole system detects every glass bottles which across the trigger switch. According to the result of impurity recognition, the alarm and control subsystem judges whether the alarm is triggered and the detected glass bottles containing impurities are ejected. The experimental flow chart is shown in Fig. 9.

The performance of the designed impurity detection system with machine learning is validated by the contrast experiments between LID (Liquid Impurity Detection) and LIDML (Liquid Impurity Detection with Machine Learning). The LID experiment and the LIDML experiment are independently in progress and the samples arrangement of the above two experiments is exactly the same. In each experiment, the system individually carries out 1000 times detection for samples in each bracket and compare the detection results (the times of each sample determined as impurity or qualification) with the presupposed arrangement of samples (the No. 1, No. 3 and No. 5 brackets are installed impurity samples, the No. 2, No. 4 and No. 6 brackets are installed qualified samples). After the last experiment, new samples are installed according to the presupposed arrangement and repeat the experiment (aggregately conducting 6 times repeated experiments), which aims to validate accuracy and stability of the detection system. The experimental results of LID are shown in Table 1 and the experimental results of LIDML are shown in Table 2.

The experimental results show that with the support of machine learning algorithm, not only the overall detection error has declined obviously, but also the stability of the detection results has significantly increased. Concretely, the weighted detection error and the weighted standard variance of the LIDML experiment (0.901% and 0.097%) are much lower than that of the LID experiment (2.772% and 0.409%). In addition, the maximum speed of the sample carrier in laboratory is 11 samples/s (39,600 samples per hour). The minimum exposure time of the industrial CCD (type: MV-GE1000M-T) is about 2.5 ms. The minimum time of analyzing a sample by IPC is about 150 ms (in the case of the industrial camera resolution ratio is adjusted to 2 million pixels). In theory, the highest detection speed of samples in the laboratory can reach to 24,000 samples per hour. However, maximum working speed of the ejection device designed by the cooperative enterprise can only reach to 10,000–12,000 samples per hour. Therefore, with a comprehensive analysis of the above detection conditions, the experiments we have conducted were carried out at the speed limit of 12,000 samples per hour. The impurity detection speed of the designed system is far greater than the traditional manual detection (3000–4000

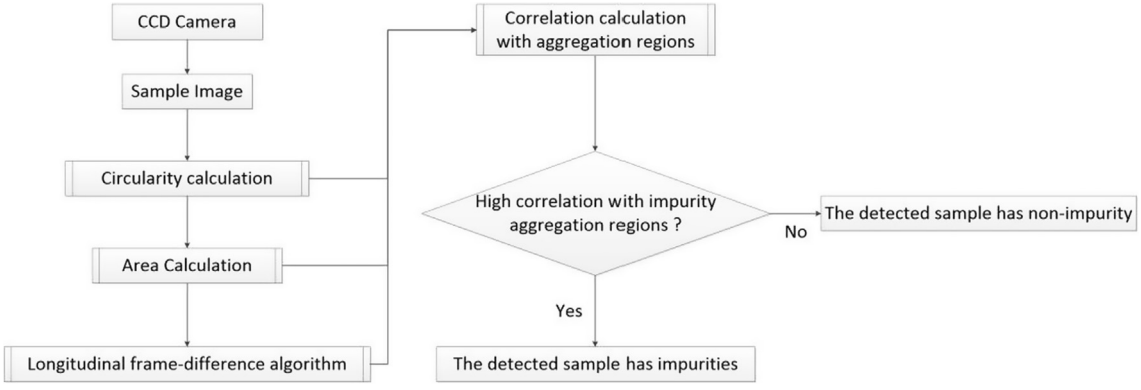

Fig. 9. The experimental flow chart.

Table 1
The experimental result of LID.

	No. 1 (Impurity)	No. 2 (Qualification)	No. 3 (Impurity)	No. 4 (Qualification)	No. 5 (Impurity)	No. 6 (Qualification)
E1	5.6%	3.3%	5.3%	2.6%	5.3%	3.0%
E2	5.0%	3.1%	4.9%	2.5%	4.8%	2.3%
E3	4.5%	2.6%	5.1%	3.3%	4.4%	2.6%
E4	4.4%	2.5%	5.3%	2.7%	5.3%	2.7%
E5	5.3%	2.4%	4.9%	2.4%	4.6%	2.8%
E6	4.7%	2.9%	4.4%	2.5%	5.0%	3.2%

E1–E6 refer to 6 times repeated experiments of the LID experiment.
No. 1–No. 6 refer to the identifier of brackets on the sample carrier.
The table parameters are the contrast error between the detection results and the presupposed arrangement of samples.
The weighted detection error (weighting ratio is 1:75) of the LID experiment is 2.772%.
The weighted standard variance of the LID experiment is 0.409%.

Table 2
The experimental result of LIDML.

	No. 1 (Impurity)	No. 2 (Impurity)	No. 3 (Impurity)	No. 4 (Qualification)	No. 5 (Impurity)	No. 6 (Qualification)
E1	1.2%	0.7%	1.5%	0.8%	1.2%	0.8%
E2	1.5%	1.2%	1.8%	0.9%	1.4%	0.7%
E3	1.6%	0.8%	1.3%	1.0%	1.3%	1.1%
E4	1.3%	0.7%	1.2%	0.9%	1.6%	0.9%
E5	1.7%	1.0%	1.4%	0.7%	1.4%	0.8%
E6	1.4%	1.1%	1.7%	1.0%	1.1%	1.0%

E1–E6 refer to 6 times repeated experiments of the LIDML experiment.
No. 1–No. 6 refer to the identifier of brackets on the sample carrier.
The table parameters are the contrast error between the detection results and the presupposed arrangement of samples.
The weighted detection error (weighting ratio is 1:75) of the LIDML experiment is 0.901%.
The weighted standard variance of the LIDML experiment is 0.097%.

Fig. 10. Contrast of impurity image between normal region and bottleneck region (a) impurity image in normal region, (b) impurity image in bottleneck region.

per hour) and the most automated detection systems (under 10,000 samples per hour). Meanwhile, with the continuous technology development of the sample ejection device, impurity detection speed of the designed system still has a large room for improvement.

5.2. Limitation analysis

With the support of machine learning algorithm, the weight detection error of the designed system is about 0.9%. However, the impurity detection error is stable at about 1.5%. The cause of the impurity detection error is much higher than the weighted error can be attributed to the phenomenon of impurities at the bottleneck of samples. Because of obvious material change at the bottleneck of samples, light may refract seriously when passing through the bottleneck. The image of impurity at the bottleneck deformed severely at the same time. It is worth noting that the orthogonal-axis inspection is difficult to eliminate such deformation. The contrast between the image of impurities in normal region and bottleneck region is shown in Fig. 10.

6. Conclusion

In this paper, a real-time detection system for impurity in bottled liquid based on machine learning is proposed. The system employs two orthogonal optical-axes HR CCD cameras to obtain undeformed visible images of detected samples. Circularity calculation combines with longitudinal frame-difference method to distinguish whether there are particular characteristics of impurities. KNN machine learning greatly improves adaptability of the system in complex environment. According to the result of detection, the system gives an alarm and ejects impurity samples controlled by PLC. Experimental results show that the proposed system has satisfactory sensitivity to dynamic and small impurities, the system has commendable capacity of resisting disturbance to interference factors such as bubbles, stains and distorted images of impurities. Meanwhile, the designed system still has a great room for improving impurity detection speed.

Acknowledgment

This work is supported by the Shanxi Province Natural Science Foundation of China (Grant No. 201601D011059).

References

[1] D.Q. Liu, M.J. Sun, L.M. Wu, Eliminating pharmaceutical impurities: recent advances in detection techniques, Curr. Opin. Drug Discov. Devel. 13 (2010) 748–757.
[2] F. Blum, High performance liquid chromatography, Br. J. Hosp. Med. 75 (2014)

C18–C21.
[3] J. Albaiges, High performance liquid chromatography in pesticide residue analysis, Int. J. Environ. Anal. Chem. 96 (2016) 1507–1508.
[4] S. Avallone, C. Renaud, B. Jacques, et al., Quantification of vitamin A in fortified oils using a fast and simple portable device: evaluation and comparison to high-performance liquid chromatography, Ann. Nutr. Metab. 63 (2013) 1101.
[5] M. Szydlowski, B. Powalka, Chatter detection algorithm based on machine vision, Int. J. Adv. Manuf. Technol. 62 (2012) 517–528.
[6] A. Laddi, S. Kumar, S. Sharma, et al., Non-invasive jaundice detection using machine vision, IETE J. Res. 59 (2013) 591–596.
[7] G. Velez, A. Moreno, D.I. Ruiz, Alvaro, et al., Real-time part detection in a virtually machined sheet metal defined as a set of disjoint regions, Int. J. Comput. Integr. Manuf. 29 (2016) 1089–1104.
[8] N. Lei, M. Soshi, Vision-based system for chatter identification and process optimization in high-speed milling, Int. J. Adv. Manuf. Technol. 89 (2017) 2757–2769.
[9] T.Z. Qiao, L.L. Chen, Y.S. Pang, et al., Integrative binocular vision detection method based on infrared and visible light fusion for conveyor belts longitudinal tear, Measurement 110 (2017) 192–201.
[10] B. Huang, J.F. Li, J.C. Wang, et al., Impurity detection using machine vision, Adv. Mater. Res. 468–471 (2012) 2057–2060.
[11] B. Huang, P. Wang, S.L. Ma, A detection system of impurity in transparent liquid, Electr. Eng. Appl. 1003 (2014) 193–197.
[12] X.L. Wen, Q.G. Xia, Y.B. Zhao, An effective genetic algorithm for circularity error unified evaluation, Int. J. Mach. Tools Manuf. 46 (2006) 1770–1777.
[13] N. Ritter, J. Cooper, New resolution independent measures of circularity, J. Math. Imaging Vision 35 (2009) 117–127.
[14] P. Bhowmick, S. Pal, Fast circular arc segmentation based on approximate circularity and cuboid graph, J. Math. Imaging Vision 49 (2014) 98–122.
[15] X.Q. Lei, C.Y. Zhang, Y.J. Xue, Roundness error evaluation algorithm based on polar coordinate transform, Measurement 44 (2011) 345–350.
[16] Y.L. Qiao, Z.M. Lu, S.H. Sun, Fast, k nearest neighbors search algorithm based on wavelet transform, IEICE Trans. Fundam. Electron. Commun. Comput. Sci. E 89A (2006) 2239–2243.
[17] J.M. Lee, Fast k-Nearest Neighbor searching in static objects, Wireless Pers. Commun. 93 (2017) 147–160.
[18] G. Biau, L. Devroye, V. Dujmovic, et al., An affine invariant k-nearest neighbor regression estimate, J. Multivariate Anal. 112 (2012) 24–34.
[19] J.Y. Jiang, S.C. Tsai, S.J. Lee, FSKNN: multi-label text categorization based on fuzzy similarity and k nearest neighbors, Expert Syst. Appl. 39 (2012) 2813–2821.
[20] Yang Kyu Shin, An improved K-means document clustering using concept vectors, J. Kor. Data Inform. Sci. 14 (2003) 853–861.
[21] L.Y. Cao, T.D. Qie, G.F. Chen, Analysis and evaluation of soil fertility status based on weighted k-means clustering algorithm, Basic Clin. Pharmacol. Toxicol. 118 (2016) 8.
[22] S.K. Sahoo, A. Makur, Dictionary training for sparse representation as generalization of K-means clustering, IEEE Signal Process Lett. 20 (2013) 587–590.